Buletin Ilmiah Sarjana Teknik Elektro
Vol. 8, No. 4, August 2026, pp. 1057-1075
ISSN: 2685-9572, DOI: 10.12928/biste.v8i4.16737

Adaptive Sliding-Mode Observer-Assisted Model Predictive Direct Speed Control for PMSM Drives Under Parameter Uncertainty and Load Disturbances

Islam Khalid [1], Othman J. Alhayali [2], Sameh Aljanabi [3]
[1] Department of Electric Power and Machine Engineering, College of Engineering, University of Diyala, Iraq
[2,3] Renewable Energy Research Center, University of Anbar, Anbar, Iraq

ARTICLE INFORMATION

Article History:

Received 14 May 2026
Revised 19 July 2026
Accepted 03 August 3036

Keywords:

PMSM;
MPDSC;
Sliding-Mode Observer;
Parameter Disturbance;
Predictive Control

Corresponding Author:

Islam Khalid,
Department of Electric Power and Machine Engineering, College of Engineering, University of Diyala, Iraq.
Email: islam.kh@uodiyala.edu.iq

ABSTRACT

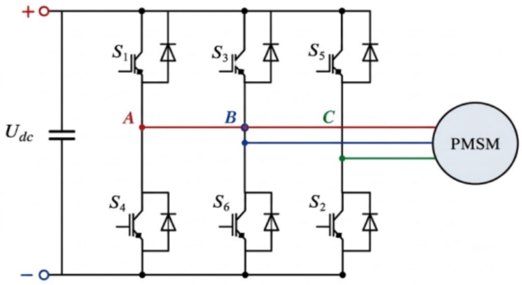

The Permanent Magnet Synchronous Motor (PMSM) drives are needed to have high dynamic accuracy and robustness under parameter uncertainty and load disturbances. Typical Model Predictive Direct Speed Control (MPDSC) techniques tend to have poor performance since the prediction accuracy is heavily dependent on the motor model. This is the main impact of this paper, which concerns the development of a real-time parameter mismatch and load disturbance estimation strategy based on the adaptive Sliding-Mode Observer (SMO) to enhance the predictive control prediction accuracy without increasing the predictive control horizon or the need for iterative optimization. The proposed adaptive SMO adaptively tunes the observer gains depending on the operating condition of the system, which enhances disturbance rejection gracefully and lessens chattering as compared with the conventional observer-based MPDSC, which uses fixed gains. The 2-level 3-phase voltage-source inverter was utilized to implement the suggested controller in MATLAB/Simulink. The predictive controller was operated with Ts = 50µs, and the current harmonic distortion was estimated by Fast Fourier Transform (FFT) analysis as per IEEE harmonic measurement practice at 1500 rpm of the steady state operating speed of the machine and 10kHz switching frequency of the inverter. The simulation results show that the performance is better under varying speed and variable-load operating conditions. The settling time of the proposed controller was reduced to 38ms as compared to 40ms for the conventional MPDSC, the current THD was reduced from 13.95% to 2.41%, the speed overshoot and torque ripple were reduced, and the disturbance rejection and tracking accuracy were improved significantly. Moreover, the adaptive observer minimized prediction errors and kept the computational structure the same as that of the conventional finite-control-set MPDSC. The results obtained in this study prove that the suggested approach is an effective and practical scheme for strong drive of PMSM.

Document Citation:

I. Khalid, O. J. Alhayali, and S. Aljanabi, "Adaptive Sliding-Mode Observer-Assisted Model Predictive Direct Speed Control for PMSM Drives Under Parameter Uncertainty and Load Disturbances," *Buletin Ilmiah Sarjana Teknik Elektro*, vol. 8, no. 4, pp. 1057-1075, 2026, DOI: 10.12928/biste.v8i4.16737.

1. INTRODUCTION

The In (PMSM) is generally utilized in systems due to its great power density, small torque ripple, and low noise [1]. Field-oriented control and direct torque control are two commonly used approaches in PMSM drive control. However, position servo systems have high requirements for dynamic performance, and the bandwidth of this cascade controller is limited [2][3]. Recently, with the continuous improvement in digital processor performance, model predictive control (MPC) has become an important means of improving system performance. Among them, finite-set MPC performs traversal optimization for an incomplete number of switching states based on the prediction model, making it easy to implement and highly flexible [4][5]. To give full play to the dynamic performance of MPC, much literature has proposed (MPDSC) methods for PMSM [6][7]. Compared with MPDSC has a simpler structure. However, existing literature rarely researches position servo systems based on MPDSC [8]. Like other forms of MPC, the control performance of MPDSC depends on the system model, involving motor electrical factors, mechanical parameters, and load torque [9]. The motor's electrical parameters will change with changing motor working conditions. The mechanical parameters cannot be directly obtained by measurement, and the measurement of load torque requires additional devices [10]. To overcome the influence of parameter uncertainty, one method is to perform online global identification of all motor parameters and load torque. The authors suggested an SMO created on a super-helical procedure for sensorless control of PMSMs. While this approach uses a fixed sliding mode coefficient, it can suppress system chattering but cannot accurately estimate the speed and rotor position [11].

Furthermore, its ability to suppress system disturbances is poor, and its robustness is weak. The authors proposed an adaptive observer approach to enhance the performance of both the controller and the observer, resulting in improved chatter suppression and interference rejection. However, the use of an adaptive observer increases the system design complexity [12][13]. The SMO is a nonlinear method created on a variable construction scheme [14]. It reduces the dependency on the system model to some degree. However, the traditional SMO may experience chattering [15], which may lead to deviations in the results. Therefore, [16] constructed a back-electromotive force observer to separate the back-electromotive force signal and suppress chattering [17]. Designed a new hybrid sliding mode observer (SMO) that achieves low chattering and implements adaptive modification of the limit layer of the sinusoidal input function through a fuzzy control system to further suppress chattering. designed a sliding mode control law in which the gain changes adaptively with the system state, thereby improving the robustness of the system [18]. Used an adaptive link to replace the filter to enhance the evaluation precision of the back-electromotive force [19]. Proposed a wide-band synchronous fundamental frequency extraction filter to extract the assessed back-electromotive force fundamental wave and improve the estimation accuracy [20]. In [21], A second-order SMO was suggested that combines the sliding mode gain of the SMO created on the super-helix procedure with the back-propagation neural network optimization and the improved phase-locked loop, which realizes the online gain adjustment and improves the dynamic response of the system. Proposes a method based on flux injection for identifying motor electrical parameters [22]. However, the additional signal injection required to introduce these parameters may impact the system's regular operation. Proposed a global factor identification scheme based on the particle swarm optimization system.

However, this biological heuristic algorithm requires iterative optimization of a great amount of data and cannot be utilized by digital processors. In addition, in the position servo system, the motor is often in a dynamic operation state, and parameter identification in a short dynamic process is still a difficulty in current research [23][24]. Another method is to compensate for factor mismatch and load disturbance based on the observer [25][26]. Among them, the SMO has received widespread attention due to its strong robustness. Proposed an SMO that can observe the mismatch of all electrical parameters [27][28]. Proposed an SMO for variable speed and variable load conditions to achieve adaptive identification of load torque [29][30]. However, motor parameter mismatch and load disturbance usually exist at the same time, and both will affect the control performance of MPDSC [31].

The suggested controller directly uses the adaptive disturbance estimates in the predictive voltage equation and the calculation of the q-axis current reference, unlike conventional MPDSC (Motor Parameter Disturbance Compensation) approaches, which use fixed motor parameters. Thus, the prediction model is updated continuously online to minimize prediction errors due to stator resistance variations, as well as load torque disturbances and uncertainty of the inductance of the prediction model. The mathematical coupling between the adaptive observer and the predictive controller is the main difference between the proposed approach and the usual observer-assisted MPDSC schemes. The characteristics and limitations of the most commonly used observer techniques are summarized in Table 1 to better emphasize the constraints of the current set of MPDSC strategies based on observer data.

1.1. Research Gap

Although significant advances have been made in both MPDSC and observer-based PMSM control solutions, there are still some key challenges. Nevertheless, the conventional MPDSC algorithms are mostly based on the fixed motor factors, and are sensitive to the differences in the electrical factors or the load disturbances. Typical back-EMF observers and conventional sliding-mode observers typically estimate only a portion of the system uncertainties and typically use a fixed observer gain, which is associated with a limitation in the rejection ability of the observer and the chattering phenomenon. While there are extended state observers and optimization-based factor identification approaches that have been suggested, they tend to increase the computational complexity or require iterative optimization, and hence are not as suited for real-time finite-control-set predictive control. Hence, there is a need for a computationally efficient predictive control scheme that is capable of compensating for parameter mismatch and load disturbances, as well as having low computational complexity, as in conventional MPDSC.

1.2. Contributions

The main research contribution of the article is to introduce a strong adaptive (SMO)-assisted (MPDSC) strategy for PMSM Drives under the condition of parameter uncertainty and load disturbances. The proposed method combines an adaptive disturbance estimation mechanism with an MPDSC approach, which does not rely on fixed-gain observers and can compensate for mismatches in the electrical parameters and external load disturbance in real time. The proposed controller directly incorporates the disturbances estimated from the model into the voltage model prediction and q-axis current reference calculation, which means that the controller can continuously improve the prediction accuracy without increasing the prediction horizon or introducing iterative optimization. Moreover, the adaptive observer gain mechanism ensures that the proposed observer does not chatter and the disturbance estimation is more accurate and robust over different operating conditions. Comprehensive MATLAB/Simulink simulations show the effectiveness of the suggested strategy, and it is validated to achieve better dynamic response, less current harmonic distortion, less torque ripple, and better disturbance rejection performance than the conventional MPDSC strategy under constant-speed, variable-speed, variable-load, and low-speed operating conditions.

Table 1. Comparison of Existing Observer Techniques

Observer Technique	Main Principle	Limitations	Effect on MPDSC
Back-EMF Observer	Estimates rotor position using back-EMF	Sensitive to parameter variations, poor low-speed performance	Reduced prediction accuracy
Conventional (SMO)	Fixed-gain sliding-mode estimation	Chattering and fixed observer gains	Limited disturbance rejection
Extended State Observer (ESO)	Estimates lumped disturbances	Higher-order observer and tuning complexity	Increased computational burden
PSO-Based Parameter Identification	Online parameter optimization	Iterative optimization and high computational cost	Unsuitable for real-time implementation
Proposed Adaptive SMO	Adaptive disturbance estimation integrated with MPDSC	Adaptive gain tuning with simultaneous parameter and load compensation	Improved prediction accuracy and robustness

2. METHODS

2.1. Mathematical Model of a PMSM

Figure 1 illustrates the topology of the three-phase PMSM servo system, based on a two-level converter, as studied in this paper [32][33]. In the d-q orientation organized system, the stator voltage and torque can be articulated as:

$$u_q = R_s * i_q + \omega_e * \Phi_d + Lq * \frac{d}{dt} iq \tag{1}$$

$$u_d = R_s * i_d - \omega_e * \Phi_q + Ld * \frac{d}{dt} id \tag{2}$$

$$T_e = \frac{3}{2} (\frac{p}{2}) (\Phi_d * i_q - \Phi_q * i_d \tag{3}$$

In the formula, u_d and u_q Are the d-axis and q-axis voltages, respectively? i_d and i_q Are the d-axis and q-axis currents, respectively; Rs is the stator resistance; L_d and L_q are the d-axis and q-axis inductances, respectively [34][35]. ω_e I_s the electrical angular velocity; Te is the electromagnetic torque; and p is the number of pole pairs. In a surface-mount PMSM, Ld=Lq=L. The mechanical equation of the PMSM can be articulated as:

$$\omega_m = \int \frac{T_e - T_L - B * \omega_m}{J} d\omega_m \tag{4}$$

Where ω_m is the mechanical angular velocity, T_L The load torque, B, is the viscous friction factor, and J is the moment of inertia.

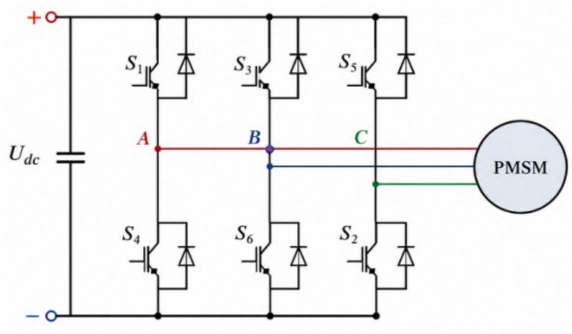

Figure 1. Topology of a three-phase PMSM based on a two-level converter

2.2. Model Predictive Direct Speed Control

Since a one-beat delay exists in digital control, it affects the system's control performance and needs to be compensated for [36][37]. When the sampling frequency is sufficiently large, the forward Euler technique can be used to discretize the motor voltage equation (1). Based on the voltage and current at time k, the current at time $k+1$ can be attained as

$$i_d(k+1) = \left(1 - \frac{R_s * Ts}{Ld}\right) i_d(k) + \left(\frac{\omega_e * Lq * Ts}{Ld}\right) i_q(k) + (\frac{Ts}{Ld})V_d \tag{5}$$

$$i_q(k+1) = \left(1 - \frac{R_s * Ts}{Lq}\right) i_q(k) - \left(\frac{\omega_e * Ld * Ts}{Lq}\right) i_d(k) + \left(\frac{Ts}{Ld}\right) V_q - \frac{\omega_r * \psi_{m*Ts}}{Lq} \tag{6}$$

Where T_s is the sampling period, ω_e The electrical angular velocity at time k, substituting equation (4) and equation (5) into the voltage discrete equation, it can obtain the voltage equation at time $k+1$ can be obtained:

$$u_d(k+1) = \left(R_s - \frac{Ld}{Ts}\right) i_d(k+1) - \omega_e * Lq * Ts\, i_q(k+1) + (\frac{Ld}{Ts}) i_d(k+1) \tag{7}$$

$$u_q(k+1) = \left(R_s - \frac{Ld}{Ts}\right) i_q(k+1) + [\omega_e * Lq * Ts\, i_d(k+1) + \psi_m] + (\frac{Ld}{Ts}) i_q(k+1) \tag{8}$$

2.3. Orientation Voltage Calculation

Substituting equation (2) into equation (3) and discretizing it yields the motor speed at time $k+1$.

$$\omega_m(k+1) = \omega_m(k) + \frac{Tsp}{J}\left[\frac{3}{2} * p * \psi_m * i_q(k+1) - Tl\right] - \frac{B * Tsp * \omega_m(k)}{J} \tag{9}$$

Because the motor's mechanical time constant is much superior to its electrical time constant, the speed sampling period Tsp is typically greater than the sampling period T_s. In this paper, $T_{sp} = 10\, T_s$. To follow the reference speed at the next moment, an MPDSC control method is used [38]. In equation (6), $\omega_m(k+1)$ is represented by ω_m^*, and $i_q(k+1)$ is represented by i_q^*. The orientation value of the q-axis current can be stated as

$$i_q^* = \frac{2}{3p * \psi_m} [\frac{J}{Tsp}\left(\omega_m^* - \omega_m(k)\right) + Tl + B * \omega_m(k)] \tag{10}$$

Using the same method, we can express $i_d(k+1)$ and $i_q(k+1)$ in equation (5) as i_d^* and i_q^*, and attain the orientation voltage at time $k+1$.

$$u_d^* = \left(R_s - \frac{Ld}{Ts}\right) i_d(k+1) - \omega_e(k) * Lq * \ i_q(k+1) + (\frac{Ld}{Ts}) i_d^* \tag{11}$$

$$u_q^* = \left(R_s - \frac{Ld}{Ts}\right) i_q(k+1) + [\omega_e(k) * Lq * i_d(k+1) + \omega_e(k) * \psi_m] + (\frac{Ld}{Ts}) i_q^* \tag{12}$$

This paper adopts the control method of $i_d^* = 0$.

2.4. Orientation Cost Function Calculation

In FCS-MPDSC, the cost function consists of two parts [39][40]. The first part is the tracking error, as shown in Equation (9). Since the reference voltage contains information about the reference speed and reference current, the speed and current can be tracked using a cost function [41][42].

$$G = (u_d^* - u_d)^2 + (u_q^* - u_q)^2 \tag{13}$$

When the motor speed satisfies the two inequalities in equation (14), it can be determined that the motor is in a steady state; otherwise, the motor is in a dynamic state. In equation (14), ω_1 Is the threshold for the absolute value of the difference between the reference speed and the actual speed. It is usually set to at least 10 times the speed fluctuation in steady state to prevent slight fluctuations in the speed in steady state from causing false switching [43][44]. ω_2 is the threshold for the absolute value of the variance between the reference speed at time k and time k-1. The value is usually selected to be of the same order of magnitude as the speed fluctuation in the steady state. When the system transitions from a steady state to a transient state, due to the change in the reference speed, the controller can promptly determine the motor's operating status and respond quickly. The switching principles of the control strategy are as follows

$$\begin{cases} |\omega_m^*(k) - \omega_m(k)| < \omega_1 \\ |\omega_m^*(k) - \omega_m^*(k-1)| < \omega_2 \end{cases} \tag{14}$$

MPDSC Strategy In a position PMSM, the motor operates in both dynamic and steady states. Figure 2 demonstrates the control block illustration of the PMSM location created on the MPSDCS strategy [45][46]. The specific steps are as follows.

(1) Compensate the controller's one-shot delay according to equation (5) and equation (6).
(2) Compute the orientation voltage according to equation (10) to equation (12).
(3) Determine the motor's operating state according to equation (14) and determine the control strategy to be adopted.
(4) Determine whether the switch state meets the control constraints, determine the value function, and select the optimal switch vector.
(5) Set the switch vector or switch vector combination for the next cycle and return to step (1).

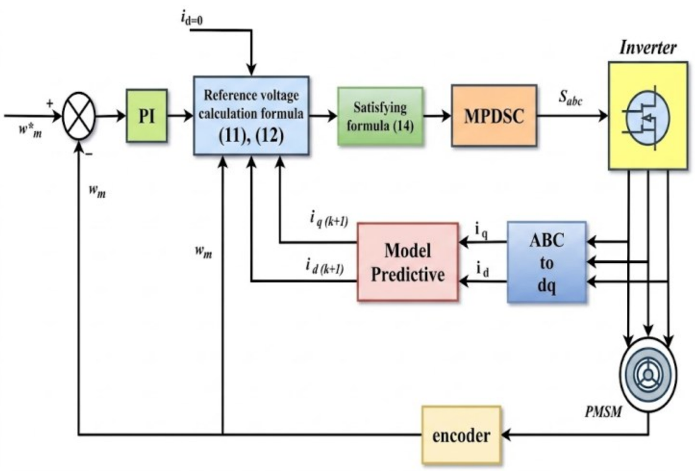

Figure 2. Block diagram based on traditional MPDSC strategy

2.5. Improved MPSDCS strategy

Figure 3 demonstrates the control block design of the improved MPDSC strategy for a PMSM position based on parameter disturbance and load observer [47][48]. To improve the robustness of MPDSC, this article suggests an SMO. A factor disturbance and burden observer is designed and created using control theory [49] [50]. Considering the system parameter mismatch and load disturbance, the d-axis and q-axis reference voltage equations and the q-axis reference current equation are shown in Equation (15):

$$u_d(k) = \left(R_s - \frac{Ld}{Ts}\right) i_d(k) - \omega_e(k) * Lq * \; i_q(k) + \left(\frac{Ld}{Ts}\right) i_d(k+1) + f_d(k) \tag{15}$$

$$F_d = \frac{f_d(k+1) - f_d(k)}{Ts} \tag{16}$$

$$u_q(k) = \left(R_s - \frac{Ld}{Ts}\right) i_q(k) + [\omega_e(k) * Lq * i_d(k) + \omega_e(k) * \psi_m] + \left(\frac{Ld}{Ts}\right) i_q(k+1) + f_q(k) \tag{17}$$

$$F_q = \frac{f_q(k+1) - f_q(k)}{Ts} \tag{18}$$

$$i_q^* = \frac{2 * J}{3p * \psi_m * Tsp}[(\omega_m(k+1) - \omega_m(k))] + \left[\frac{2 * (Tl + B * \omega_m(k))}{3p * \psi_m}\right] + f_\omega(k) \tag{19}$$

$$f_\omega(k) = \frac{f_\omega(k+1) - f_\omega(k)}{Ts} \tag{20}$$

Where f_d, f_q, and f_ω Represent the sum of the disturbances due to factor mismatch and load, and F_d, F_q, and F_ω , represent the rate of change of the disturbance. u_{dSMO}, u_{qSMO}, and $u_{\omega SMO}$ These are the SMC functions. The SMO surface and SMO convergence rate are defined as follows:

$$\begin{gathered} S_d = i_d^* - i_d(k) \\ S_q = i_q^* - i_q(k) \\ S_q = \omega_m^* - \omega_m(k) \end{gathered} \tag{21}$$

$$\begin{gathered} \frac{dS_d}{dt} = -A_d|S_d|sign(S_d) \\ \frac{dS_q}{dt} = -A_q|S_q|sign(S_q) \\ \frac{dS_\omega}{dt} = -A_\omega|S_\omega|sign(S_\omega) \end{gathered} \tag{22}$$

Where A_d, A_q, and A_ω are the convergence rate parameters, and sign () represents the sign function. The SMO function can be considered as follows:

$$\begin{gathered} u_{dSMO} = L\, A_d|S_d(k)|sign(S_d(k)) - R_s S_d(k) \\ u_{qSMO} = L\, A_q|S_q(k)|sign\left(S_q(k)\right) - R_s S_q(k) \\ u_{\omega SMO} = \frac{2J}{3p * \psi_m}[\, A_\omega|S_\omega(k)|sign(S_\omega(k)) - \frac{2BS_d(k)}{3p * \psi_m} \end{gathered} \tag{23}$$

Based on the equation (23) parameter disturbance and load torque observer, the q-axis reference current and reference voltage can be compensated in real time. The compensated q-axis reference current and reference voltage are shown below:

$$\widehat{i_q^*} = \frac{2 * J}{3p * \psi_m * Tsp}\left[\left(\omega_m^* - \widehat{\omega_m}(k)\right)\right] + \left[\frac{2 * (Tl + B * \widehat{\omega_m}(k))}{3p * \psi_m}\right] * f_\omega(k+1) \quad (24)$$

$$\widehat{u_d^*} = \left(R_s - \frac{Ld}{Ts}\right)\widehat{i_d}(k+1) - \widehat{\omega_e}(k) * Lq * \widehat{i_q}(k+1) + \left(\frac{Ld}{Ts}\right)\widehat{i_d^*} + \widehat{f_d}(k+1) \quad (25)$$

$$\widehat{u_q^*} = \left(R_s - \frac{Ld}{Ts}\right)\widehat{i_q}(k+1) + \left[\omega_e(k) * Lq * \widehat{i_d}(k+1) + \widehat{\omega_e}(k) * \psi_m\right] + \left(\frac{Ld}{Ts}\right)\widehat{i_q^*} + \widehat{f_q}(k+1) \quad (26)$$

Finally, the parameter disturbance and load torque observer can be articulated as shadows.

$$\widehat{i_d}(k+1) = \left(1 - \frac{R_s * Ts}{Ld}\right)\widehat{i_d}(k) + \left(\frac{\omega_e(k) * Lq * Ts}{Ld}\right)i_q(k) + \left(\frac{Ts}{Ld}\right)u_d(k) - \left(\frac{Ts}{Ld}\right)\widehat{f_d}(k) + \left(\frac{Ld}{Ts}\right)u_{dSMO} \quad (27)$$

$$\widehat{f_d}(k+1) = K_d * u_{dSMO} * Ts + \widehat{f_d}(k) \quad (28)$$

$$\widehat{i_q}(k+1) = \left(1 - \frac{R_s * Ts}{Lq}\right)\widehat{i_q}(k) - \left(\frac{\omega_r * Ld * Ts}{Lq}\right)i_d(k) + \left(\frac{Ts}{Ld}\right)u_q(k) - \frac{\omega_r * \psi_{m*Ts}}{Lq} - \left(\frac{Ts}{Ld}\right)\widehat{f_q}(k) - \left(\frac{Ts}{Ld}\right)u_{qSMO} \quad (29)$$

$$\widehat{f_q}(k+1) = K_q * u_{qSMO} * Ts + \widehat{f_q}(k) \quad (30)$$

$$\widehat{\omega_m}(k+1) = \omega_m(k) + \frac{3 * Tspp * \psi_m *}{2J}\left[\widehat{i_q}(k+1) - \widehat{f_\omega}(k) - u_{\omega SMO}\right] - \frac{B * Tsp * \omega_m(k) + Tl * Tsp}{J} \quad (31)$$

$$\widehat{f_\omega}(k+1) = K_\omega * u_{\omega SMO} * Tsp + \widehat{f_\omega}(k) \quad (32)$$

Where K_d, K_q, and $K_\omega$are sliding mode parameters

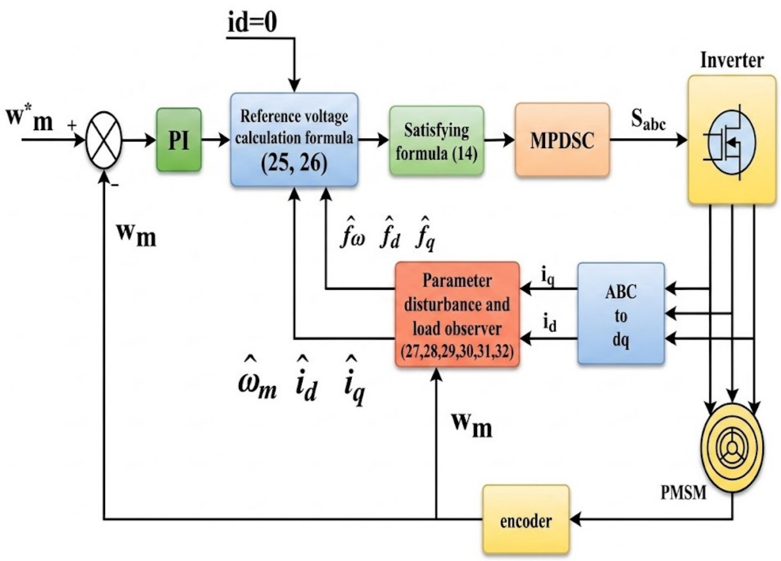

Figure 3. Block diagram based on improved MPDSC strategy

2.6. Research Methodology Flowchart

The research methodology is illustrated in Figure 4, detailing the development of an (MPDSC) framework for a three-phase (PMSM). It begins with mathematical modeling, followed by the addition of an adaptive (SMO) for real-time assessment of electrical parameter mismatches and load disturbances. This estimation enhances prediction accuracy and disturbance rejection by compensating for the predictive voltage model and q-axis current reference. The methodology employs a finite-control-set objective function to limit the optimal inverter switching state for controlling the (VSI) of the PMSM. Effectiveness is demonstrated through MATLAB/Simulink simulations across various conditions, including variable-speed, variable-load, and low-speed scenarios.

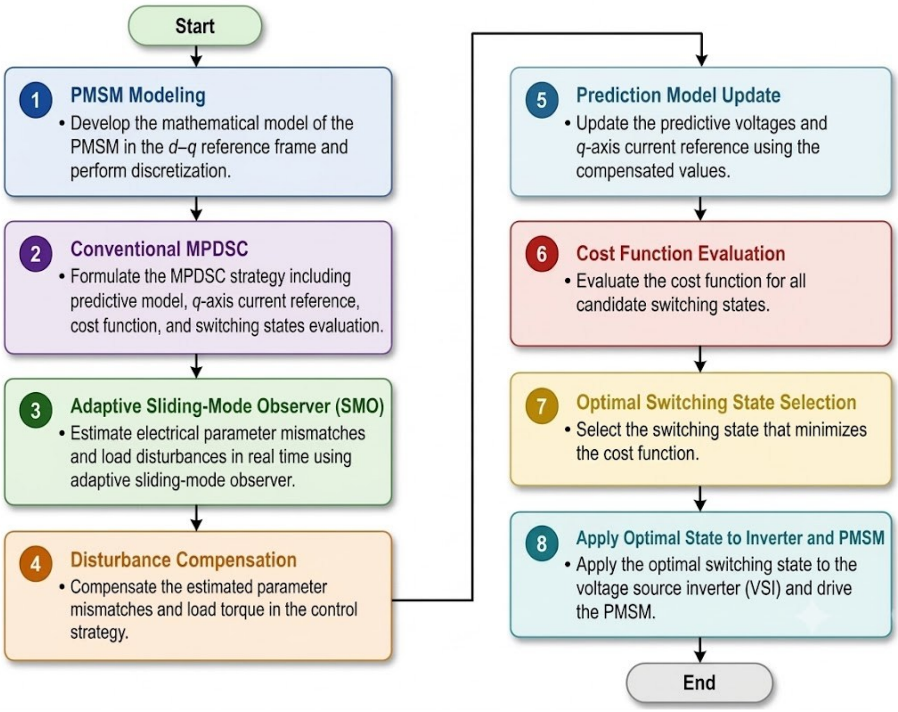

Figure 4. Shows the proposed research methodology

2.7. Stability Analysis of the Suggested Adaptive SMO

A Lyapunov stability analysis is carried out to check the convergence and stability of the suggested adaptive SMO. Define estimation errors of the d-axis current, q-axis current, and speed as the corresponding sliding surfaces S_d, S_q, and S_ω defined in equation (19) to equation (22), respectively. The adaptive sliding-mode control laws are specified in (23), and the disturbance observer update equations are defined in equation (27) to equation (32) and their dynamics are governed by the observer. The quadratic Lyapunov candidate function is chosen as

$$V = \frac{1}{2}\left(S_d^2 + S_q^2 + S_\omega^2\right) \tag{33}$$

Taking the time derivative of (33) gives

$$\dot{V} = S_d\dot{S}_d + S_q\dot{S}_q + S_\omega\dot{S}_\omega \tag{34}$$

By replacing the adaptive sliding mode control laws of (23) into the error dynamics, it is found that the adaptive SMO laws can ensure that the error dynamics are

$$\dot{V} = -A_d \mid S_d \mid -A_q \mid S_q \mid -A_\omega \mid S_\omega \mid +\Delta(t) \tag{35}$$

The bounded uncertainty $\Delta(t)$ due to parameter mismatches and external load disturbances. The adaptive gains A_d, A_q, and A_ω are chosen so that.

$$A_i > \Delta_{\max}, i = d, q, \omega \tag{36}$$

The Lyapunov derivative is satisfied as shown below:

$$\dot{V} < 0, \forall (S_d, S_q, S_\omega) \neq 0 \quad (37)$$

Based on Lyapunov's direct stability theorem, the sliding surfaces tend to vanish asymptotically,

$$\lim_{t\to\infty} S_d = \lim_{t\to\infty} S_q = \lim_{t\to\infty} S_\omega = 0 \quad (38)$$

This guarantees stable estimation of the parameter disturbances and load torque. Thus, the compensated reference current and voltage equations expressed by equation (24) to equation (26) always minimize the prediction error for the MPDSC algorithm and enhance the robustness of the control against disturbances.

2.8. Computational Complexity Analysis

The proposed adaptive SMO-assisted (MPDSC) approach aims to enhance the disturbance rejection capabilities while maintaining the computational efficiency of the existing finite-control-set MPDSC algorithm. The proposed method at each sampling interval checks the same set of a finite number of inverter switching states, while the optimization-based predictive controllers need to use iterative numerical optimization or an extended prediction horizon. Thus, the computational structure of the predictive controller remains the same. This extra computation arises because of the implementation of the Adaptive (SMO) that is used to estimate the mismatches between the electrical parameters and the load disturbances in real-time. The primary computations are algebraic operations and observer update equations for which matrix inversion and iterative optimization are not necessary. This means that the computation time is not too high and can be used in real time. Table 2 shows the computational complexity of the conventional and proposed MPDSC strategies.

Table 2. Computational complexity comparison

Operation	Conventional MPDSC	Proposed Adaptive SMO-MPDSC
Prediction model evaluation	8	8
Cost function evaluations	8	8
Observer update equations	0	6
Additional multiplications	0	18
Additional additions	0	15
Matrix inversion	No	No
Iterative optimization	No	No
Prediction horizon	One-step	One-step
Real-time implementation	Yes	Yes

3. RESULT AND DISCUSSION

To ratify and ideate the control strategy that has been projected and discussed within the boundaries of this scholarly item, an advanced testing platform amounting to a two-level three-state Permanent Magnet Synchronous Motor (PMSM) was meticulously designed and assembled to facilitate exact exploratory reasoning. Furthermore, the various imitation limits that pertain particularly to the conduct and functional characteristics of the PMSM under search are completely itemized and presented in a smooth plan, which may be about Table 3, through providing critical insights into the engine's behavior under various functional environments.

Table 3. Shows PMSM parameters

Parameter	Values
Rs	1.3Ω
Lq=Ld	0.009H
Pole Pairs	3
Flux	0.41Wb
Udc	300V
K_d, K_q, and K_ω	0.4,3.245,2.35

3.1. Case 1 is When the Speed is Constant and the Load Changes From 0 to 5 to 10

This system was tested at constant speed and variable load, with the reference speed being 1500 rpm. The speed response shown in Figure 5 is identical to the reference speed, but the overshoot is high under load conditions. When the speed was fixed, and the load increased as shown in Figure 5 from 0 to 5 and 10 Nm, the speed response showed a high-speed disturbance in cases of load change. At a time of 5s, it led to a speed decrease of 1475. Furthermore, at 15 seconds, it led to an increase in speed, reaching 1530. Using the traditional MPDSC strategy, the position access time is about 40ms, at times 5 s, or 15 s.

The estimated position error of the conventional approach called MPDSC is illustrated as a waveform in Figure 6. It is remarkable to note that the size of the error estimate is quite considerable, which suggests that there could be some issues with the control strategy used. At 5s, an error is observed that has a strong overshoot of 28 units, and at 15s, the error is observed again and is a strong -30 units. In addition, there is a significant variation or ripple in the estimation of error, indicating some instability in the system's reaction. This difference in the error dynamics may hurt the process control system's performance and reliability. Therefore, it is important to further investigate these error characteristics for improved overall effectiveness of the MPDSC approach.

During the motor operation phase, in terms of speed and error, the fluctuations under MPDSC improved, while the fluctuations under the are small. When the speed was fixed, and the load increased as shown in Figure 7, from 0 to 5 and 10 Nm, the speed response showed a low-speed disturbance in cases of load change. At a time of 5s, it led to a speed decrease of 1490. Also, at a time of 15s, it led to an increase in speed reaching 1512. Using the improved MPDSC strategy, the position access time is about 38ms, at times 5s and 15s.

Figure 8 shows the waveform equivalent to the guessed position error for the embellished (MPDSC) methods. The belief in mistakes is the least. At the 5-second mark, the error is noticed to exhibit an omission of 10, and at the 15-second mark, the omission is written as -12. The ripple in the wrong direction is slight.

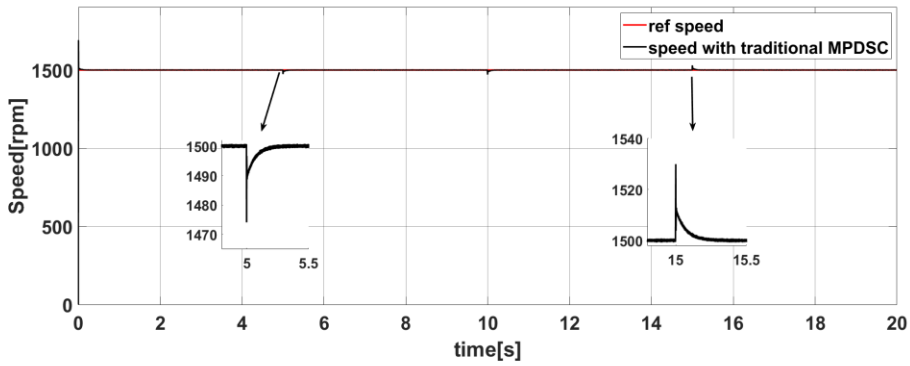

Figure 5. Speed with conventional MPDSC

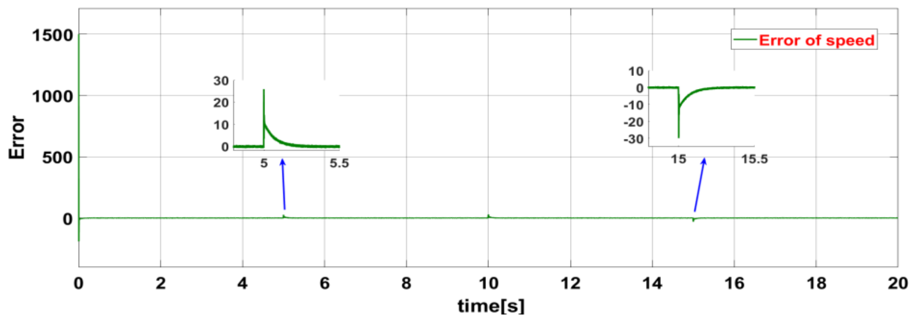

Figure 6. Speed error with conventional MPDSC

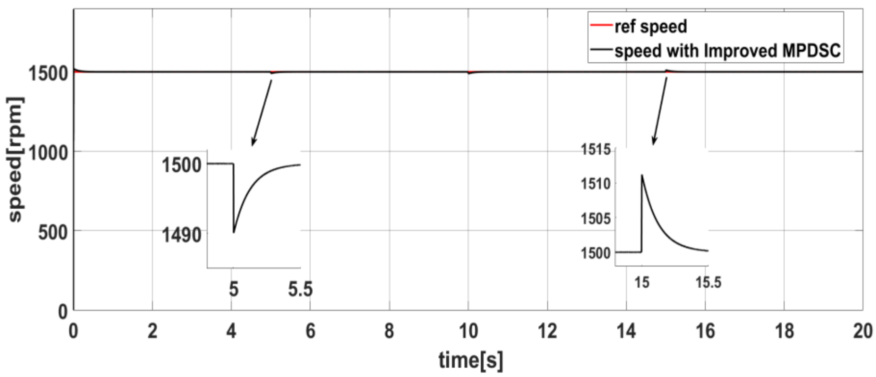

Figure 7. Speed with improved MPDSC

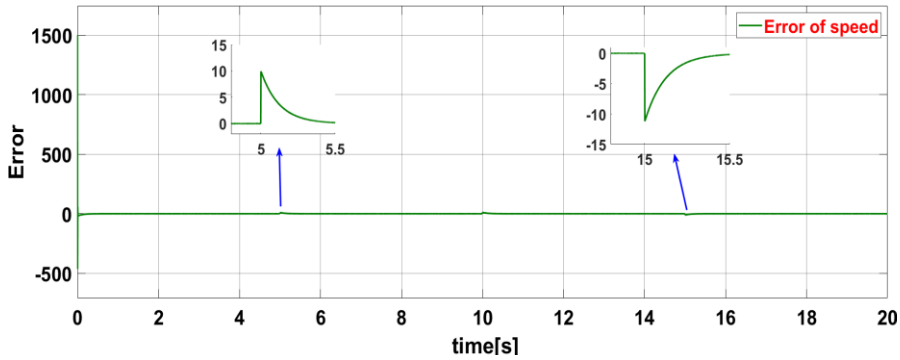

Figure 8. Speed error with improved MPDSC

3.2. Case 2 is When the Load is Constant, and the Speed Changes

When the load is held constant, and the rotational speed is augmented as depicted in Figure 9 from 0 to 200 to 400 to 900 and 1500 rpm at the respective time intervals of [0 0.1 0.11 4 4.1 8 8.1 12 12.1 20.5] seconds, the response in speed exhibits significant fluctuations, ultimately achieving stabilization after 40 milliseconds. The speed error is shown as shown in Figure 10. The overshoot is significant, and the oscillations in the error are significant too. The error is seen to have an overshoot of 2.58 at the time mark of 4 seconds and becomes 5.2 at 12 seconds.

When the load remains constant, and the speed is increased as shown in Figure 11 from 0 to 200 to 400 to 900 and 1500 rpm at times [0 0.1 0.11 4 4.1 8 8.1 12 12.1 20.5] seconds respectively, the speed response shows low fluctuations and stabilizes after 35ms. Figure 12 shows the speed error. The overshoot and the ripple in the error are small. At 4 s, the error is seen to be an overshoot of 0.27, and at 12 s, the overshoot is 0.9. The MPDSC optimization significantly improves the dynamic stability quality of the PMSM system, effectively enhancing the system's performance and verifying the feasibility of this approach.

Figure 13 shows the stator current of the traditional MPDSC. The fluctuations of the current are large, and the ripple is high. To further analyze the impact of motor factor changes on the transient performance of the stator three-phase current (iabe), a fast Fourier transform analysis (FFT) of phase A current was performed. At the same switching frequency, Figure 14 shows that the THD of the traditional MPDSC is 13.95%. Conventional control has a ripple current waveform and a higher pulse. The FFT analysis was carried out for the rated operating condition with a fundamental electrical frequency of 75 Hz. The harmonic spectrum has been calculated for the fundamental stator current component, and the presented values of THD were derived from it.

Figure 15 illustrates that the stator current waveform of the improved MPDSC is as close as possible to the sinusoidal waveform, and the latter controller exhibits a smoother current waveform, less pulsation, and better motor stability. Also, MPDSC improved the no-overshoot. At the same switching frequency, Figure 16 displays that the THD of the MPDSC improved to 2.41%. Improved control has a low ripple current waveform and a low pulse. The FFT analysis was carried out for the rated operating condition with a fundamental electrical frequency of 75 Hz. The harmonic spectrum has been calculated for the fundamental stator current component, and the presented values of THD were derived from it.

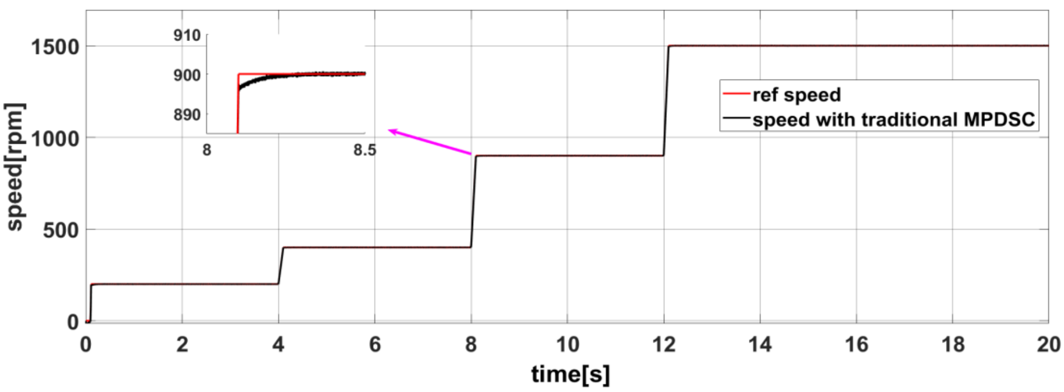

Figure 9. Speed with conventional MPDSC

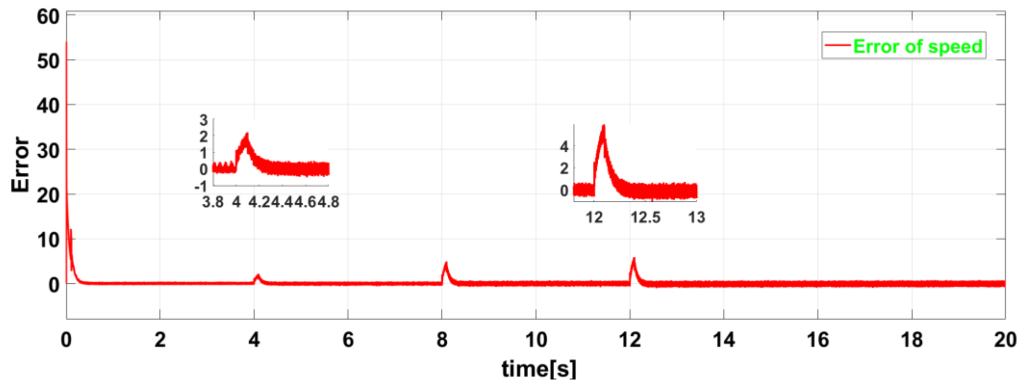

Figure 10. Speed error with conventional MPDSC

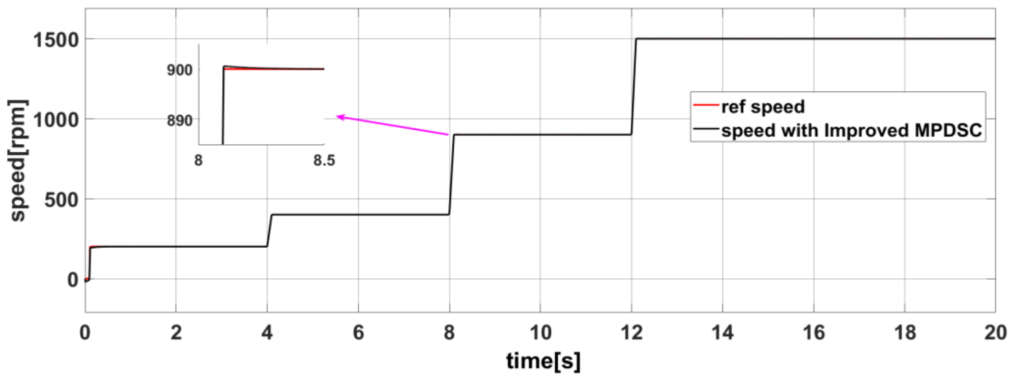

Figure 11. Speed with improved MPDSC

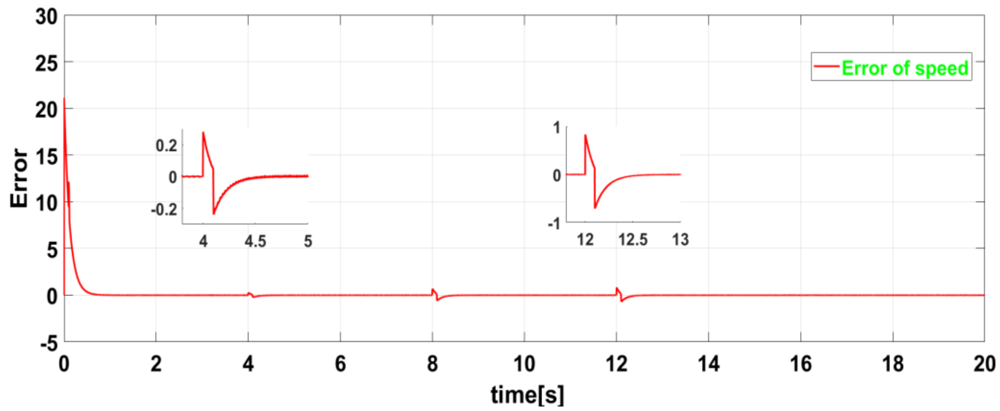

Figure 12. Speed error with improved MPDSC

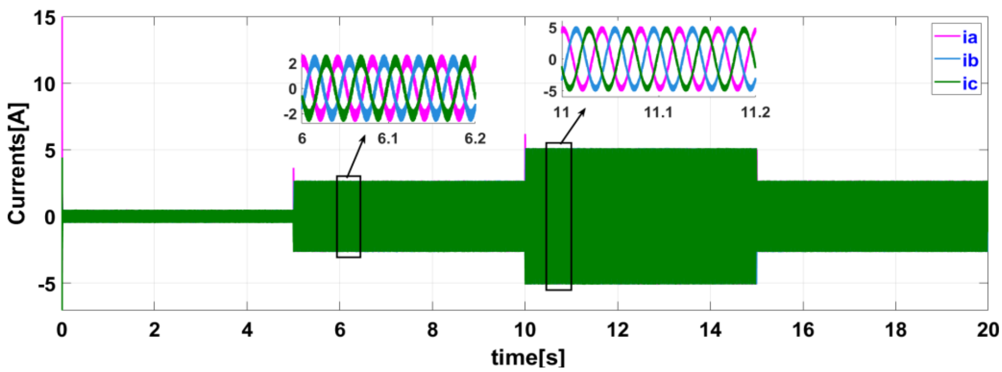

Figure 13. 3-Phase Currents with the MPDSC conventional

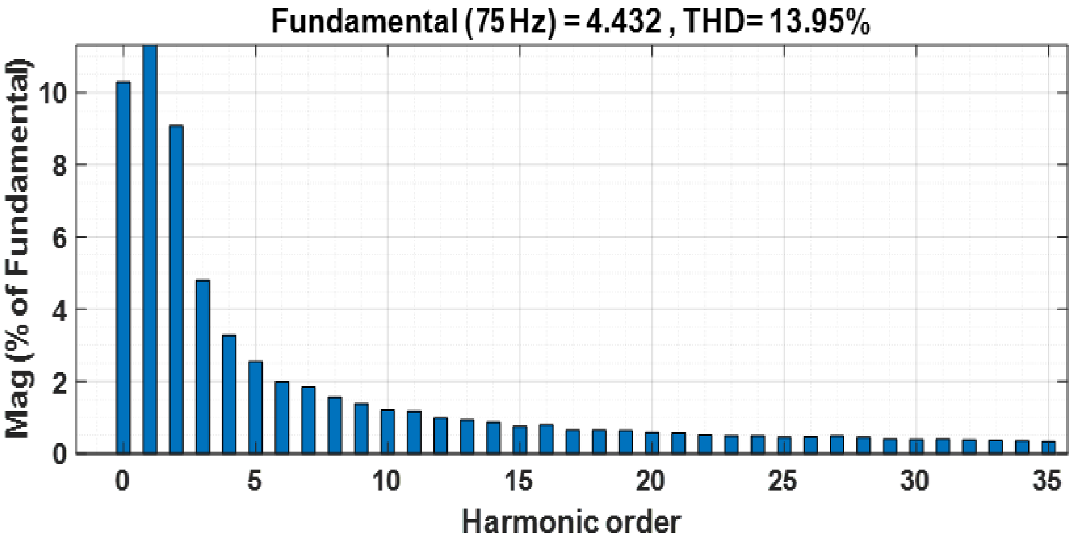

Figure 14. Displays the THD with the MPDSC conventional

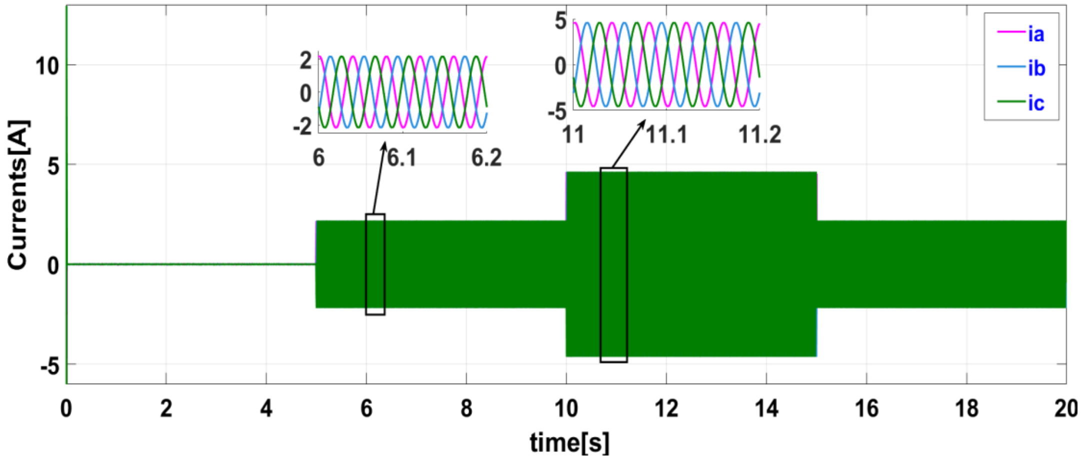

Figure 15. 3-Phase Currents with the improved MPDSC

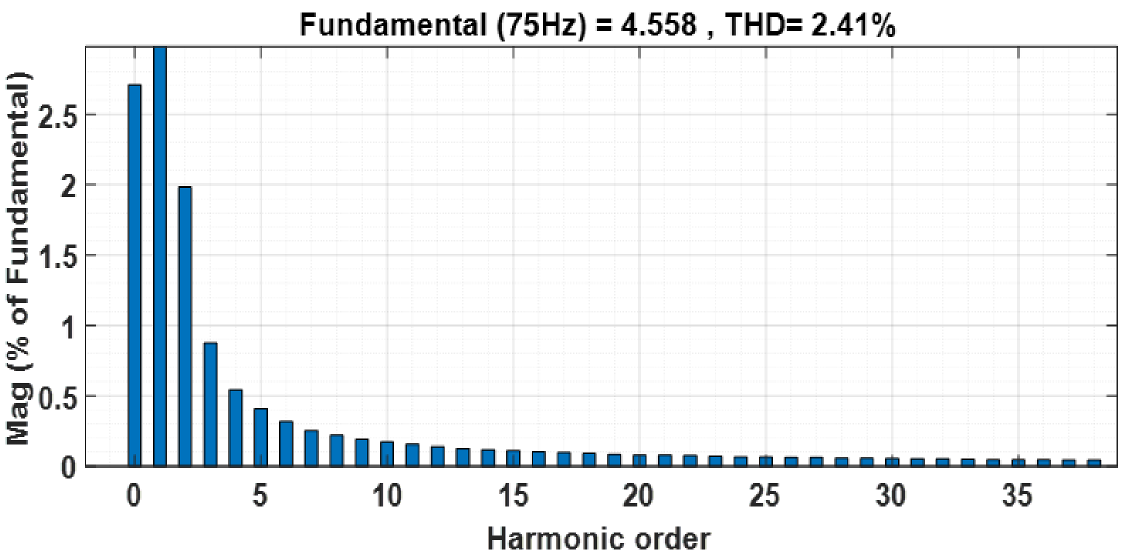

Figure 16. Shows the THD with the improved MPDSC

3.3. Case 3 is When the Load Changes, and the Low-Speed Changes

The speed response has some fluctuation when the speed and load change. This is shown in Figure 17 and Figure 18 at low speed. The improved method has little overshoot and ripple. The introduction of the MPDSC optimization has an important impact on the dynamic stability of the PMSM system, which can further enhance the performance of the system and verify the feasibility of this technique.

The electromagnetic torque (T_e) responses of the PMSM drive to variable load conditions are shown in Figure 19 and Figure 20, respectively corresponding to the standard MPDSC and the suggested adaptive SMO-assisted MPDSC. The actual developed electromagnetic torque is shown as a red curve, while the reference electromagnetic torque (T_e, ref) is displayed as a blue curve in both figures. The conventional MPDSC can track the reference torque, but it is found that the torque oscillations are noticeable after load variations caused by factor mismatch and external disturbances, as demonstrated in Figure 19. Overall, the adaptive SMO-assisted MPDSC delivers much smoother torque tracking with quicker recovery, as shown in Figure 20, and much lower torque ripple under the same operating conditions. The better performance is due to the adaptive sliding-mode observer, which is continuously estimating and compensating for the uncertainty of the parameters and load disturbances, which increases the accuracy of the prediction of the MPDSC algorithm. From a quantitative point of view, the proposed controller also results in a reduction of torque ripple from about 27% (conventional MPDSC) to about 3% (proposed controller), thus confirming the superior dynamic response, robustness, and steady-state torque regulation.

Table 4 lists the main quantitative performance metrics of the conventional MPDSC as well as the proposed adaptive SMO-assisted MPDSC. The proposed controller offers a significant decrease in current THD (from 13.95% to 2.41%) and torque ripple (from 27% to 3%), and at the same time reduces the settling time (40ms to 38ms), and improves speed tracking performance under load disturbances. The proposed disturbance compensation mechanism is effective, as evidenced by these combined improvements.

Table 5 quantitatively compares the conventional MPDSC and the proposed Adaptive SMO-assisted MPDSC. While the increase in settling time is relatively small (40ms to 38ms), the proposed controller also provides a large amount of reduction in the current THD and torque ripple, as well as better disturbance rejection and steady state stability. The proposed adaptive disturbance compensation mechanism has been shown to enhance the transient and steady state control performance, as the combined improvements are shown.

The qualitative comparison of the proposed adaptive SMO-assisted MPDSC scheme with some of the representative observer-based PMSM control schemes reported in the literature is shown in Table 6. Despite its simplicity, conventional MPDSC has been shown to have poor performance levels when handling parameter uncertainties and load disturbances. The observer-based methods, like Modified Flux SMO and Load Adaptive SMO, enhance the accuracy of estimation but are mainly used for operation without any sensors or parameter estimation. Also, ADRC-based strategies demonstrate good disturbance rejection properties, but they also typically use control structures that differ. Unlike the current controller, however, the proposed controller incorporates an adaptive sliding-mode observer, which allows parameter mismatch errors and load disturbance errors to be simultaneously compensated and retains the computational convenience of one-step predictive control. These attributes are seen in the better current THD, improved speed tracking, and greatly reduced torque ripple that have been achieved in the present study.

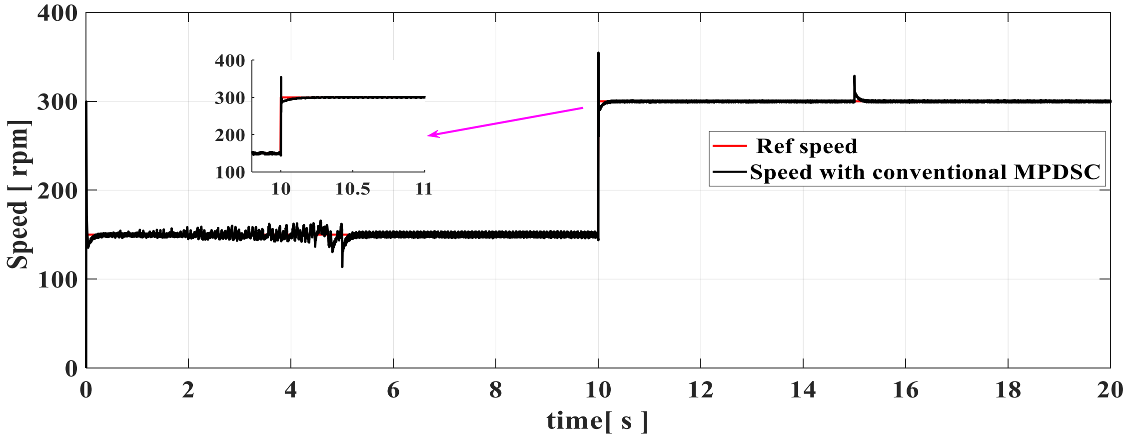

Figure 17. Speed with conventional MPDSC

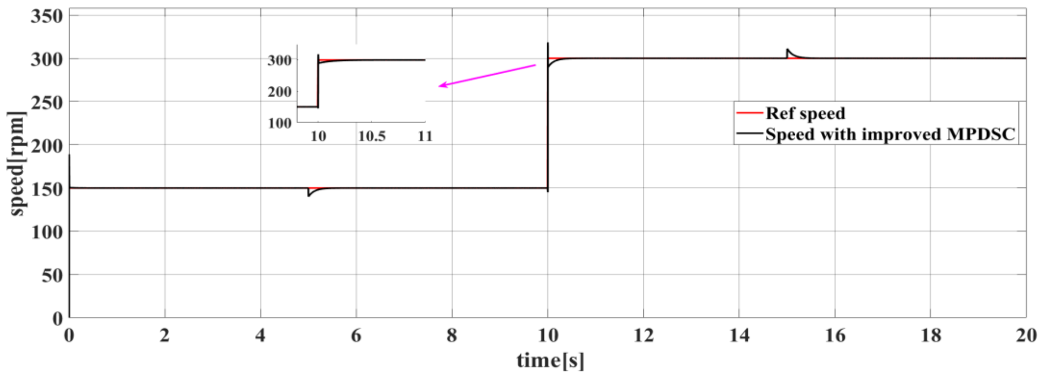

Figure 18. Speed with improved MPDSC

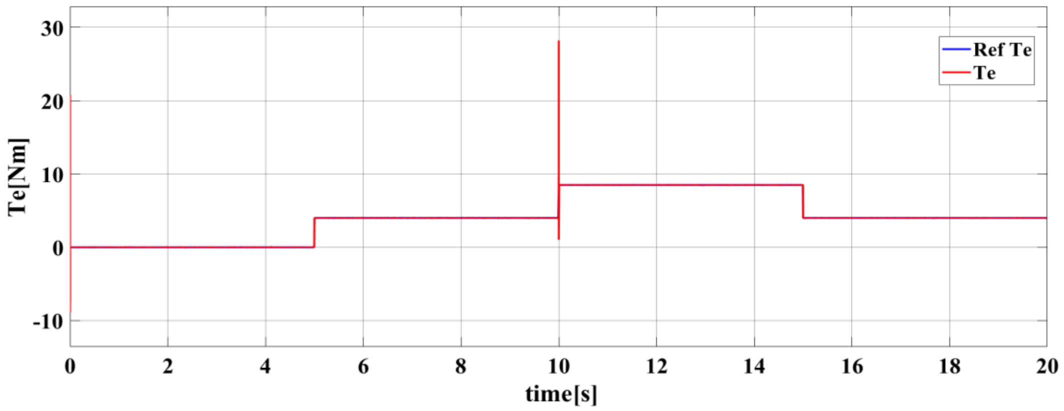

Figure 19. Torque with improved MPDSC

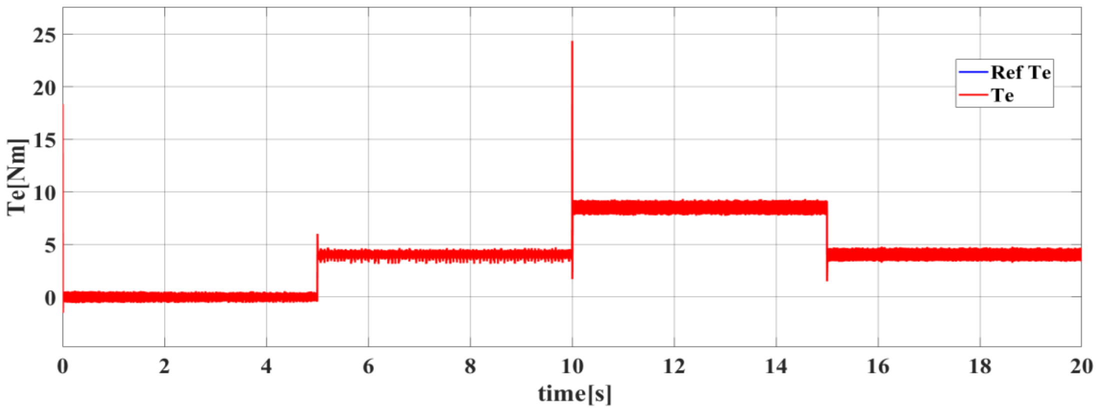

Figure 20. Torque with conventional MPDSC

Table 4. Lists the main quantitative performance

Performance Index	Conventional MPDSC	Proposed
Settling Time (ms)	40	38
Current THD (%)	13.95	2.41
Torque Ripple (%)	27	3
Speed Tracking	Moderate	Excellent
Disturbance Rejection	Moderate	Excellent

Table 5. Quantitative Performance Comparison

Performance Index	Conventional MPDSC	Proposed Adaptive SMO-Assisted MPDSC	Improvement
Speed Tracking	Good	**Excellent**	Improved
Disturbance Rejection	Moderate	**Excellent**	Improved
Steady-State Stability	Good	**Excellent**	Improved

Table 6. Compares the proposed controller with recent observer-based PMSM controllers qualitatively.

Method	Main Characteristics	Limitations	Comparison with the Proposed Method
ADRC-Based PMSM Control [21][23]	Excellent disturbance rejection through active disturbance estimation.	Higher controller complexity does not exploit the finite-control-set predictive control framework.	The proposed method preserves the MPDSC structure while providing online disturbance compensation with lower implementation complexity.
Modified Flux SMO [25]	Online estimation of stator resistance and inductance improves sensorless operation.	Primarily focuses on parameter estimation and does not directly compensate for simultaneous electrical parameter mismatch and load disturbances within the predictive controller.	The proposed adaptive SMO simultaneously estimates parameter disturbances and load torque while directly enhancing MPDSC prediction accuracy.
Load-Adaptive SMO [31]	An adaptive observer improves load estimation and dynamic response under varying operating conditions.	Observer performance depends on adaptive tuning and is mainly designed for position servo applications.	The proposed method integrates adaptive SMO with MPDSC to improve disturbance rejection and predictive speed control under both parameter uncertainties and load variations.
Proposed Adaptive SMO-Assisted MPDSC	Adaptive estimation of parameter mismatch and load disturbance combined with finite-control-set MPDSC.	Simulation validation only; experimental implementation remains future work.	Achieves improved speed tracking, disturbance rejection, lower current THD (2.41%), and reduced torque ripple (3%) while maintaining the simplicity of one-step predictive control.

4. CONCLUSIONS

In this paper, an adaptive (SMO)-assisted (MPDSC) approach for PMSM drives under parameter uncertainties and load disturbances is presented. The proposed controller has successfully incorporated an adaptive disturbance observer into the predictive control structure, which ensures that the electrical parameter mismatches and external load disturbances are compensated for at all times, thereby enhancing the prediction accuracy and disturbance rejection. Simulation results showed that the proposed strategy could reduce the settling time from around 40ms to 38ms, the stator current THD from 13.95% to 2.41%, and the torque ripple from 27% to 3% without any loss of the accurate speed tracking under the varying speed and varying load operating conditions. The results display that the suggested adaptive observer can enhance the robustness and dynamic performance of the MPDSC strategy without iterative optimization or increasing the prediction horizon. However, there are some drawbacks to the proposed approach. No experimental testing has been conducted on a real PMSM drive, and the controller has only been tested through MATLAB/Simulink simulations. Additionally, the adaptive observer requires proper gain tuning, and the extra observer calculations are not negligible and must be tested on embedded hardware platforms. Further, the variations in the thermal parameters and possible measurement errors, under actual operating conditions, could also influence the performance of the observers. Thus, experimental implementation on DSP/FPGA platforms, Hardware-in-the-Loop (HIL) validation, automatic observer gain tuning, and comprehensive real-time performance evaluation in realistic operational situations will be the key areas of future work.

Author Contribution

The main contribution to this paper was made by all of the authors. All the authors have read and approved the final article.

Acknowledgement

The authors are thankful to the lecturers at the University.

Conflicts of Interest

The authors have no conflict of interest to declare.

REFERENCES

[1] L. Wogi, M. Morawiec, and T. Ayana, "Sensorless Control of Induction Motor Based on Super-Twisting Sliding Mode Observer With Speed Convergence Improvement," *IEEE Access*, vol. 12, no. May, pp. 74239–74250, 2024, https://doi.org/10.1109/ACCESS.2024.3404040.

[2] Y. Yang, S. C. Tan, and S. Y. R. Hui, "Adaptive Reference Model Predictive Control with Improved Performance for Voltage-Source Inverters," *IEEE Trans. Control Syst. Technol.*, vol. 26, no. 2, pp. 724–731, 2018, https://doi.org/10.1109/TCST.2017.2670529.

[3] M. K. Ismael, S. T. Bahar, and A. A. Abdullah, "Harmonic Elimination Method for Permanent Magnet Synchronous Motor Utilizing Active Disturbance Rejection Control," *Proc. Eng. Technol. Innov.*, vol. 30, pp. 11–23, 2025, https://doi.org/10.46604/peti.2024.14386.

[4] S. Abood, A. Annamalai, I. Khalid, M. Chouikha, and H. A. Al-Zuhairi, "AI-Based Hybrid Control for Optimizing Doubly-Fed Induction Generators in Wind Turbines," *Int. J. Intell. Eng. Syst.*, vol. 18, no. 6, pp. 439–459, 2025, https://doi.org/10.22266/ijies2025.0731.28.

[5] Y. Zhang, S., Wang, Y., Hu, and Y. Zhang, "Model Predictive Control with Parameter Robustness for Surface-mounted Permanent Magnet Synchronous Motor Drives," in *2021 IEEE International Conference on Predictive Control of Electrical Drives and Power Electronics (PRECEDE)*, pp. 322–327, 2021, https://doi.org/10.1109/precede51386.2021.9680908.

[6] H. Wang, S. Zhang, W. Liu, Q. Geng, and Z. Zhou, "Finite control-set model predictive direct speed control of a PMSM drive based on the Taylor series model," *IET Electric Power Applications*, vol. 15, no. 11, pp. 1452–1465, July 2021, https://doi.org/10.1049/elp2.12112.

[7] S. T. Bahar and H. Qiu, "Amelioration of Traditional PI Boost Converter Utilizing Linear Active Disturbance Rejection Controller-Mode Predictive Control Strategy," *Int. J. Robot. Control Syst.*, vol. 6, no. 1, pp. 305–323, 2026, https://doi.org/10.31763/ijrcs.v6i1.2364.

[8] S. T. Bahar, W. Wang, and H. Qiu, "AI-Enhanced Model Predictive and Active Disturbance Rejection Control for High-Performance Permanent Magnet Synchronous Motor Drives," *Energies*, vol. 19, no. 11, p. 2574, May 2026, https://doi.org/10.3390/en19112574.

[9] Z. Chen, L., Chen, J., Qiu, L., Shi, D., and Qi, D., "Current Sampling Scheme for Finite-Control-Set Model Predictive Control of PMSM Drives with Two Shunt Resistors," in *2023 IEEE International Conference on Predictive Control of Electrical Drives and Power Electronics (PRECEDE)*, pp. 1–6, 2023, https://doi.org/10.1109/precede57319.2023.10174466.

[10] B. R. Park, G. C. Lim, J. Choi, C. Hwang, and J.-I. Ha, "Torque Ripple Minimization of PMSM Drive with Speed Ripple Feedback Considering Non-linearities of PMSM," in *2021 IEEE Energy Conversion Congress and Exposition (ECCE)*, 2021, https://doi.org/10.1109/ecce47101.2021.9595926.

[11] S. T. Bahar and Raed A. Abd-Alhmeed, "Reduce-Complexity of Predictive Current 479 Control for a 3-Phase Voltage Source Inverter," *Journal of Techniques*, vol. 7, no. 3, pp. 480 16–25, Sep. 2025, https://doi.org/10.51173/jt.v7i3.2621.

[12] S. Zhuo, A. Gaillard, L. Guo, L. Xu, D. Paire, and F. Gao, "Active Disturbance Rejection Voltage Control of a Floating Interleaved DC-DC Boost Converter with Switch Fault Consideration," *IEEE Trans. Power Electron.*, vol. 34, no. 12, pp. 12396–12406, 2019, https://doi.org/10.1109/TPEL.2019.2905897.

[13] S. Masoudi and H. Mehrjerdi, "A Multilayer Perception Trained Method in Speed Control of a Linear Switched Reluctance Motor," *IEEE Transactions on Power Electronics*, vol. 37, no. 4, pp. 4475-4483, 2022, https://doi.org/10.1109/TPEL.2021.3125606.

[14] R. K. Chillab and H. A. Hasan, "Adaptive Hybrid Fuzzy–Neural PID Control of Speed Regulation and Torque Ripple Reduction of BLDC Motors", *Buletin Ilmiah Sarjana Teknik Elektro*, vol. 8, no. 3, pp. 792–810, Jun. 2026, https://doi.org/10.12928/biste.v8i3.16182.

[15] Y. Zhao, L. Ren, Z. Liao, and G. Lin, "A Novel Model Predictive Direct Torque Control Method for Improving Steady-State Performance of the Synchronous Reluctance Motor," Energies, vol. 14, no. 8, p. 2256, 2021, https://doi.org/10.3390/en14082256.

[16] X. Li, Y. Cui, and X. Wu, "Sensorless Control of Surface-Mounted Permanent Magnet Synchronous Motor in a Wide-Speed Range," *Electron.*, vol. 13, no. 6, 2024, https://doi.org/10.3390/electronics13061131.

[17] N. K. Quang and Q. P. Ha, "FPGA-based Sensorless PMSM Drive with Sliding Mode Observer for Velocity Tracking," *IEEE Access*, vol. 14, no. March, pp. 39687–39701, 2026, https://doi.org/10.1109/ACCESS.2026.3673003.

[18] N. V. Laksmi B., M. S. Mubarok, W. Aribowo, D. Purwanto, J. R. Isaac, and V. H. Abdullayev, "Indirect Matrix Converter Based Synchronous Reluctance Motor Drive Systems using Model Predictive Control", *Buletin Ilmiah Sarjana Teknik Elektro*, vol. 8, no. 2, pp. 331–343, Mar. 2026, https://doi.org/10.12928/biste.v8i2.15222.

[19] K. Wang, R. D. Lorenz, and N. A. Baloch, "Enhanced Methodology for Injection-Based Real-Time Parameter Estimation to Improve Back EMF Self-Sensing in Induction Machine Deadbeat-Direct Torque and Flux Control Drives," IEEE Trans. Ind. Appl., vol. 54, no. 6, pp. 6071–6080, 2018, https://doi.org/10.1109/TIA.2018.2855162.

[20] Q. H. Le and N. T. Pham, "Predefined-Time Super-Twisting Disturbance-Observer-Based Speed Control for PI-Based FOC Induction Motor Drives", *Buletin Ilmiah Sarjana Teknik Elektro*, vol. 8, no. 2, pp. 451–462, Apr. 2026, https://doi.org/10.12928/biste.v8i2.15761.

[21] Z. Hao *et al.*, "Linear/Nonlinear Active Disturbance Rejection Switching Control for Permanent Magnet Synchronous Motors," *IEEE Trans. Power Electron.*, vol. 36, no. 8, pp. 9334–9347, 2021, https://doi.org/10.1109/TPEL.2021.3055143.

[22] C. LIU, G. LUO, Z. CHEN, W. TU, and C. QIU, "A linear ADRC-based robust high-dynamic double-loop servo system for aircraft electro-mechanical actuators," *Chinese J. Aeronaut.*, vol. 32, no. 9, pp. 2174–2187, 2019, https://doi.org/10.1016/j.cja.2019.03.036.

[23] M. Tian, B. Wang, Y. Yu, Q. Dong, and D. Xu, "Discrete-Time Repetitive Control-Based ADRC for Current Loop Disturbances Suppression of PMSM Drives," *IEEE Trans. Ind. Informatics*, vol. 18, no. 5, pp. 3138–3149, 2022, https://doi.org/10.1109/TII.2021.3107635.

[24] Q. Zhang, Y. Fan, and C. Mao, "A Gain Design Method for a Linear Extended State Observers to Improve Robustness of Deadbeat Control," *IEEE Trans. Energy Convers.*, vol. 35, no. 4, pp. 2231–2239, 2020, https://doi.org/10.1109/TEC.2020.3009119.

[25] S. Ye and X. Yao, "A Modified Flux Sliding-Mode Observer for the Sensorless Control of PMSMs with Online Stator Resistance and Inductance Estimation," *IEEE Trans. Power Electron.*, vol. 35, no. 8, pp. 8652–8662, 2020, https://doi.org/10.1109/TPEL.2019.2963112.

[26] A. B. Badri, I. K. A. Razzaqe, and O. A. Kadhim, "AI-Driven Predictive Maintenance for Rare-Earth-Free Synchronous Motors in Smart Grid Applications," *Mathematical Modelling of Engineering Problems*, vol. 13, no. 1, pp. 99–110, Feb. 2026, https://doi.org/10.18280/mmep.130110.

[27] Z. Wu, D. Li, Y. Liu, and Y. Q. Chen, "Performance Analysis of Improved ADRCs for a Class of High-Order Processes With Verification on Main Steam Pressure Control," *IEEE Trans. Ind. Electron.*, vol. 70, no. 6, pp. 6180–6190, 2023, https://doi.org/10.1109/TIE.2022.3192687.

[28] J. She, M. Xie, D. Y. Li, M. Wu, Z. T. Liu, and W. N. Zhang, "A VFF-RLS Method of Inertia Identification for PMSM," *CCTA 2019 - 3rd IEEE Conf. Control Technol. Appl.*, no. 10, pp. 942–943, 2019, https://doi.org/10.1109/CCTA.2019.8920489.

[29] H. Dan, W. Yue, W. Xiong, Y. Liu, M. Su and Y. Sun, "Open-Switch and Current Sensor Fault Diagnosis Strategy for Matrix Converter-Based PMSM Drive System," *IEEE Transactions on Transportation Electrification*, vol. 8, no. 1, pp. 875-885, 2022, https://doi.org/10.1109/TTE.2021.3109093.

[30] X. Wang *et al.*, "Well-Conditioned Identifiability Criteria With Observability Degree for Parameter Estimation of Permanent Magnet Synchronous Motors," *IEEE Transactions on Transportation Electrification*, vol. 11, no. 3, pp. 7195-7206, 2025, https://doi.org/10.1109/TTE.2024.3524783.

[31] W. Lu, B. Tang, K. Ji, K. Lu, D. Wang, and Z. Yu, "A New Load Adaptive Identification Method Based on an Improved Sliding Mode Observer for PMSM Position Servo System," *IEEE Trans. Power Electron.*, vol. 36, no. 3, pp. 3211–3223, 2021, https://doi.org/10.1109/TPEL.2020.3016713.

[32] S. T. Bahar and R. G. Omar, "Permanent Magnet Synchronous Motor Torque Ripple Reduction Using Predictive Torque Control," J. Eng. Sustain. Dev., vol. 27, no. 3, pp. 394–406, 2023, https://doi.org/10.31272/jeasd.

[33] W. Zhang, W. Wang, H. Liu, and D. Xu, "A Disturbance Rejection Control Strategy for Droop-Controlled Inverter Based on Super-Twisting Algorithm," *IEEE Access*, vol. 7, no. c, pp. 27037–27046, 2019, https://doi.org/10.1109/ACCESS.2019.2900501.

[34] Z. H. Liu, H. L. Wei, X. H. Li, K. Liu, and Q. C. Zhong, "Global Identification of Electrical and Mechanical Parameters in PMSM Drive Based on Dynamic Self-Learning PSO," *IEEE Trans. Power Electron.*, vol. 33, no. 12, pp. 10858–10871, 2018, https://doi.org/10.1109/TPEL.2018.2801331.

[35] X. Zhang, B. Hou, and Y. Mei, "Deadbeat Predictive Current Control of Permanent-Magnet Synchronous Motors with Stator Current and Disturbance Observer," *IEEE Trans. Power Electron.*, vol. 32, no. 5, pp. 3818–3834, 2017, https://doi.org/10.1109/TPEL.2016.2592534.

[36] J. M. Tabora *et al.*, "Exploring the Effects of Voltage Variation and Load on the Electrical and Thermal Performance of Permanent-Magnet Synchronous Motors," *Energies*, vol. 17, no. 1, p. 8, 2023, https://doi.org/10.3390/en17010008.

[37] Y. Zhao, W. Qiao, and L. Wu, "Improved Rotor Position and Speed Estimators for Sensorless Control of Interior Permanent-Magnet Synchronous Machines," *IEEE Journal of Emerging and Selected Topics in Power Electronics*, vol. 2, no. 3, pp. 627–639, 2014, https://doi.org/10.1109/JESTPE.2014.2298433.

[38] T. T. Pham and N. T. Pham, "A Hybrid PI–SOSM Control Strategy with Disturbance Observer for Enhanced Dynamic Response of IM Drives", *Buletin Ilmiah Sarjana Teknik Elektro*, vol. 7, no. 4, pp. 702–714, Oct. 2025, https://doi.org/10.12928/biste.v7i4.14458.

[39] F. Xie *et al.*, "The Optimal Speed-Torque Control of Asynchronous Motors for Electric Cars in the Field-Weakening Region Based on the RFR," *IEEE Trans. Ind. Electron.*, vol. 67, no. 11, pp. 9601–9612, 2020, https://doi.org/10.1109/TIE.2019.2956379.

[40] B. Guo, S. Bacha, M. Alamir, A. Hably, and C. Boudinet, "Generalized Integrator-Extended State Observer with Applications to Grid-Connected Converters in the Presence of Disturbances," *IEEE Trans. Control Syst. Technol.*, vol. 29, no. 2, pp. 744–755, 2021, https://doi.org/10.1109/TCST.2020.2981571.

[41] A. Najem, A. Moutabir, A. Ouchatti, and M. E. Haissouf, "Experimental Validation of the Generation of Direct and Quadratic Reference Currents by Combining the Ant Colony Optimization Algorithm and Sliding Mode Control in PMSM using the Process PIL," *International Journal of Robotics and Control Systems*, vol. 4, no. 1, pp. 188–216, Mar. 2024, https://doi.org/10.31763/ijrcs.v4i1.1286.

[42] X. Zhang, Z. Zhao, Y. Cheng, Y. Wang, "Robust Model Predictive Current Control Based on Inductance and Flux Linkage Extraction Algorithm," *IEEE Transactions on Vehicular Technology*, vol. 69, no. 12, pp. 14893-14902, 2020, https://doi.org/10.1109/TVT.2020.3043474.

[43] Z. Guoqing *et al.*, "Research on Position Sensorless Control of PMSM Based on Improved SMO," *IOP Conf. Ser. Mater. Sci. Eng.*, vol. 533, no. 1, 2019, https://doi.org/10.1088/1757-899X/533/1/012019.

[44] M. Nicola, C. I. Nicola, D. Selișteanu, and D. Șendrescu, "PMSM Sensorless Control System Based on Super Twisting-Terminal SMC and SMO-PLL Observer," *2024 28th Int. Conf. Syst. Theory, Control Comput. ICSTCC 2024 - Proc*., no. 1, pp. 483–490, 2024, https://doi.org/10.1109/ICSTCC62912.2024.10744709.

[45] E. J. Fuentes, C. A. Silva, and J. I. Yuz, "Predictive speed control of a two-mass system driven by a permanent magnet synchronous motor," *IEEE Trans. Ind. Electron*., vol. 59, no. 7, pp. 2840–2848, 2012, https://doi.org/10.1109/TIE.2011.2158767.

[46] P. G. Carlet, A. Favato, S. Bolognani, F. Dorfler, "Data-Driven Continuous-Set Predictive Current Control for Synchronous Motor Drives," *IEEE Transactions on Power Electronics*, vol. 37, no. 6, pp. 6637–6646, 2022, https://doi.org/10.1109/TPEL.2022.3142244.

[47] H. H. Lee, P. Q. Dzung, L. D. Khoa, and L. M. Phuong, "The optimized adaptive space vector pulse width modulation for four switch three phase inverter under DC - Link voltage ripple condition," *IEEE Reg. 10 Annu. Int. Conf. Proceedings/TENCON*, no. 2, pp. 1–6, 2009, https://doi.org/10.1109/TENCON.2009.5396098.

[48] J. Liu and H. Yu, "Active Disturbance Rejection Control of SEA Based on Reduced Order Extended State Observer," *Lect. Notes Electr. Eng.*, vol. 885 LNEE, no. 2, pp. 121–129, 2022, https://doi.org/10.1007/978-981-19-1309-9_12.

[49] M. S. Rafaq and J. W. Jung, "A Comprehensive Review of State-of-the-Art Parameter Estimation Techniques for Permanent Magnet Synchronous Motors in Wide Speed Range," *IEEE Trans. Ind. Informatics*, vol. 16, no. 7, pp. 4747–4758, 2020, https://doi.org/10.1109/TII.2019.2944413.

[50] Z. H. Liu, H. L. Wei, Q. C. Zhong, K. Liu, X. S. Xiao, and L. H. Wu, "Parameter estimation for VSI-Fed PMSM based on a dynamic PSO with learning strategies," *IEEE Trans. Power Electron*., vol. 32, no. 4, pp. 3154–3165, 2017, https://doi.org/10.1109/TPEL.2016.2572186.